Full paper / Mémoire

Block copolymers for corrosion protection of aluminium

Vincent Roche [a,b], Florence Vacandio [a,*], Denis Bertin [b], Didier Gigmes [b], Marielle Eyraud [a]

[a] *Laboratoire Chimie Provence (UMR 6264), Équipe « Électrochimie des matériaux », Centre Saint-Jérôme,
avenue Escadrille-Normandie-Niemen, 13397 Marseille cedex 20, France*
[b] *Laboratoire Chimie Provence (UMR 6264), Équipe « Chimie radicalaire, organique et polymères de spécialité »,
Centre Saint-Jérôme, avenue Escadrille-Normandie-Niemen, 13397 Marseille cedex 20, France*

Abstract

In this work, poly(*n*-butyl acrylate-*b*-trifluoroethyl methacrylate) (PBA-*b*-PTFEMA) and poly(*n*-butyl acrylate-*b*-heptadeca-fluorodecyl methacrylate) (PBA-*b*-PHFEMA) diblock copolymers synthesized by controlled radical polymerisation are used as a monolayer to protect aluminium against corrosion.

Contact angle measurements show hydrophobic behaviour that can be attributed to the presence of a fluorinated block. The preferential orientation of the fluorinated block at the coating/air interface can explain the high hydrophobicity behaviour. Finally, corrosion resistance has been investigated by Electrochemical Impedance Spectroscopy (EIS). The results show that the PBA-*b*-PHFEMA copolymer provides excellent anti-corrosion barrier properties, even after 60 days of immersion in a solution of 3% NaCl. *To cite this article: V. Roche et al., C. R. Chimie 11 (2008).*
© 2008 Académie des sciences. Published by Elsevier Masson SAS. All rights reserved.

Résumé

Des copolymères à blocs poly(acrylate de *n*-butyl-*b*-méthacrylate trifluoroéthyle) (PBA-*b*-PTFEMA) et poly(acrylate de *n*-butyl-*b*-méthacrylate d'heptadécafluorodécyle) (PBA-*b*-PHFEMA) ont été synthétisés par polymérisation radicalaire contrôlée. Ces polymères ont été par la suite appliqués en revêtement monocouche afin de protéger l'aluminium contre la corrosion. La morphologie des revêtements obtenus a été caractérisée par microscopie à force atomique (AFM). Par la suite, leur caractère hydrophobe, dû à la présence du bloc fluoré, a été mis en évidence par mesures d'angles de contact. Les résultats ont montré l'orientation préférentielle du bloc fluoré à l'interface revêtement/air, expliquant leur caractère fortement hydrophobe. Enfin, leur résistance à la corrosion a été étudiée par spectroscopie d'impédance électrochimique (SIE). Il en ressort que le copolymère PBA-*b*-PHFEMA présente d'excellentes propriétés de barrière anticorrosion, même après 60 jours d'immersion dans une solution de NaCl 3%. *Pour citer cet article : V. Roche et al., C. R. Chimie 11 (2008).*
© 2008 Académie des sciences. Published by Elsevier Masson SAS. All rights reserved.

* Corresponding author.
E-mail address: florence.vacandio@univ-provence.fr (F. Vacandio).

1. Introduction

Most of the time, protection of metallic substrates (e.g., aluminium, steel, galvanised steel…) against corrosion by organic coatings involves multilayer systems. These systems include at least three painting layers of different types: the primary layer — directly applied on the substrate — confers a good adhesion on the system of painting, an intermediate layer, which generally provides the thickness of the coating and its barrier function, and finally, the topcoat to protect all the underlying layers. This layer often brings the esthetical aspect. Each painting layer is usually formulated from five constituents [1–4]: the binder matrix (usual binders are epoxy, polyurethane or alkyde), inorganic or metallic pigments, extenders, additives for specific properties (anti-foamers, fire retarding agents, anti-coalescence agents, UV-absorbers…) and solvents (to reduce the viscosity of the coating and to control the drying).

The major disadvantage of the use of these three coat-painting systems is related to the coating process (time and cost). In order to simplify the sequence, the key step is to elaborate a single layer (unilayer system) gathering all properties of a three-layer-based system. To reach this objective, various properties of polymers (low water permeability, good mechanical properties…) have been combined using diblock copolymer as a monocomponent system (Fig. 1).

In a diblock copolymer, the two segments are covalently bonded [5]. The presence of covalent bonds between the blocks definitely improves the mutual miscibility of the two polymers. Thus, a nanoscale self-organization can be easily achieved for such
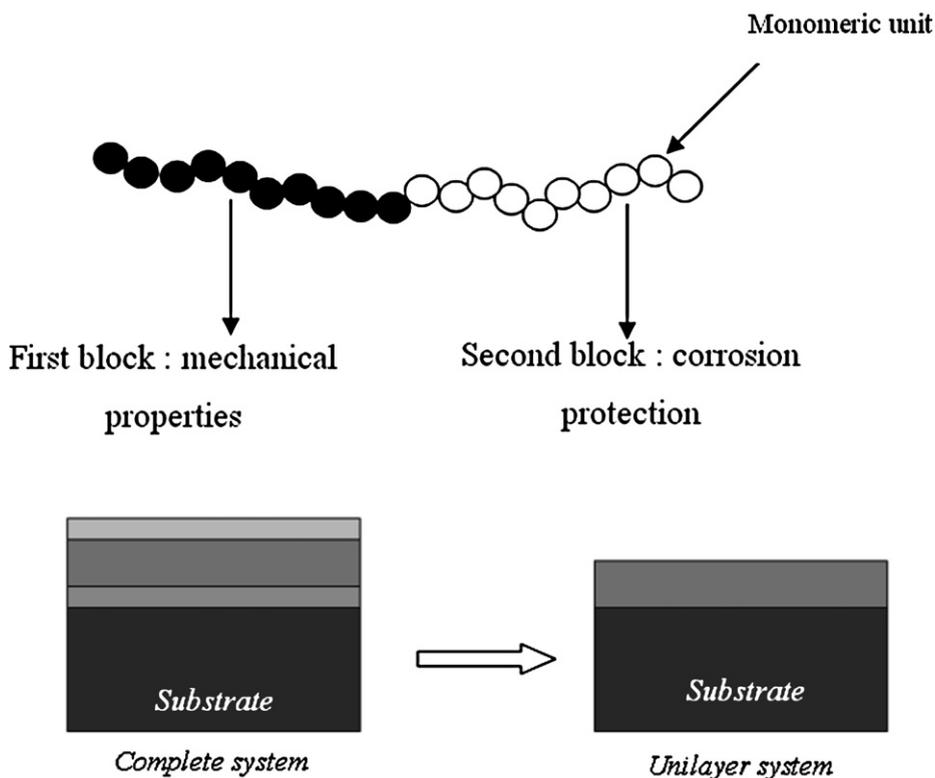

Fig. 1. Schematic representations of a block copolymer and a system of paintings.

copolymers (not for statistical copolymers). Various nanostructures could be obtained from sphere, cylinder, bicontinuous to lamellae organization, which are mainly governed by the composition of the diblock copolymer [6].

In this work, we have studied the protection of Al substrates against corrosion using two types of unilayer systems based on block copolymers that have been synthesized using the NMP technique (Nitroxide-Mediated Polymerisation) [7,8]. In both cases, the first block (poly(*n*-butyl acrylate) (PBA)) has been chosen for its amorphous and elastomer properties and the second block, consisting of a fluorinated polymer, has been selected for its rigidity and its good water impermeability. The difference between the two block copolymers is the nature of the fluorinated block:

(1) poly(*n*-butyl acrylate-*b*-trifluoroethyl methacrylate) diblock copolymer (PBA-*b*-PTFEMA) (Fig. 2a);
(2) poly(*n*-butyl acrylate-*b*-heptadecafluorodecyl methacrylate) diblock copolymer (PBA-*b*-PHFEMA) (Fig. 2b).

2. Experimental

2.1. Synthesis of copolymers

All monomers were purchased from Aldrich and used as received. BlocBuilder™ was provided by Arkema company.

2.1.1. PBA-b-PTFEMA diblock copolymer

This diblock copolymer was elaborated by NMP (Nitroxide-Mediated Polymerisation). *n*-Butyl acrylate monomers (BAs) (3.1×10^{-1} mol) and BlocBuilder™ alcoxyamine initiator (2.0×10^{-3} mol) (Fig. 3) were charged in a glass reactor provided with a cooler and an inflow of sluggish gas (N_2). The medium of polymerisation is deoxygenated by nitrogen bubbling during 20 min and placed under magnetic stirring in a thermostated oil bath and then heated from room temperature to 110 °C. After the removal of residual
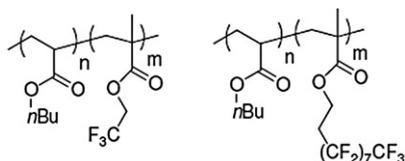

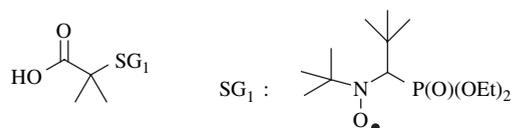Fig. 2. (a) PBA-*b*-PTFEMA diblock copolymer, (b) PBA-*b*-PHFEMA diblock copolymer.

Fig. 3. BlocBuilder™ alkoxyamine initiator.

monomer under reduced pressure, PBA block ($M_n = 14{,}200$ g/mol, calculated by SEC) was used as a macro-initiator to synthesise the PTFEMA block ($M_n = 8570$ g/mol, calculated by ^{1}H NMR). The procedure is similar (n(PBA) $= 6.1 \times 10^{-4}$ mol and n(TFEMA) $= 6.9 \times 10^{-2}$ mol), but is performed at 90 °C. Finally, the monomer is eliminated by stripping under reduced pressure.

2.1.2. PBA-b-PHFEMA diblock copolymer

This diblock copolymer was elaborated by NMP. The procedure is similar to that of the PBA-*b*-PTFEMA synthesis. *n*-Butyl acrylate monomers (3.9×10^{-1} mol) (BA) and BlocBuilder™ alkoxyamine initiator (3.0×10^{-3} mol) were charged in a glass reactor provided with a cooler and an inflow of sluggish gas (N_2). After purification, the obtained PBA block ($M_n = 13{,}900$ g/mol, calculated by SEC) was used as a macro-initiator to synthesise the PHFEMA block ($M_n = 23{,}950$ g/mol, calculated by ^{1}H NMR). The diblock copolymer was purified by precipitation in pentane.

2.2. Elaboration of coatings

Prior to film deposition, aluminium panels (3105 H24) (6.5 cm × 6.5 cm) were successively cleaned in acetone and ethanol using an ultrasonic rinse and then dried under airflow. PBA-*b*-PTFEMA and PBA-*b*-PHFEMA films were deposited using a three-step sequence: dissolution of the copolymer in a solvent (tetrahydrofuran for PBA-*b*-PTFEMA copolymer and 1,3 bis-trifluoromethyl benzene for PBA-*b*-PHFEMA copolymer), deposition of the solution obtained (450 mg/mL) on the substrate with an automatic bar coater and evaporation of the solvent. After solvent evaporation (1 h in air), the coatings were annealed at 120 °C during 24 h.

A Positector 6000 Defelsko and an FNS2 Defelsko probe have been used to estimate the thicknesses of coatings that have been found to be in the 90 ± 2 μm range.

2.3. Atomic force microscopy (AFM)

AFM images of the samples and the corresponding average surface roughness measurements were

obtained using an Autoprobe CP (Park Scientific Instrument) in non-contact mode. All observations were performed in "Topographic Mode". All AFM measurements were carried out in air at 25 °C with a standard silicon nitride cantilever.

2.4. Contact angle measurements

For the determination of the surface free energy of the coating, selected test liquids, with different γ_{sl} for a common solid, depending upon the dispersion and dipolar interaction of the liquids, were utilized. For reliable determination of the surface free energy, different test liquids are usually preferred, as indicated in Table 1. A "KRUSS" EasyDrop contact-angle measuring system was employed. Each test liquid was placed (3 μL) on the sample using an automatic syringe. The baseline is measured automatically and the angle is determinated between the baseline of the drop and the tangent at the drop. The corresponding free energy of the coating has been calculated by means of the Owens−Wendt method [9], in which the polar and dispersive parts of the surface free energy are obtained by plotting the $(1 + \cos\theta)\gamma_l/2(\gamma_l^d)^{1/2}$ versus $(\gamma_l^p)^{1/2}/(\gamma_l^d)^{1/2}$. The slope of the fitted line and the intercept gives $(\gamma_s^p)^{1/2}$ and $(\gamma_s^d)^{1/2}$, respectively.

2.5. Electrochemical characterization

The electrochemical characterization was performed using a traditional three-electrode electrochemical cell with a platinum grid as counterelectrode and a saturated calomel electrode (SCE) as reference electrode. The Electrochemical Impedance Spectroscopy tests were carried out in a 3 wt% sodium chloride solution at open-circuit potential, with a 20 mV amplitude signal, a frequency range from 10^5 to 10^{-2} Hz for further measurements. All electrochemical experiments were performed with a frequency response analyser (Solartron 1260) connected to a potentiostat (Solartron 1287). In order to perform accurate measurements, the electrochemical cell was placed in a Faraday cage.

Table 1
Surface free energy of the test liquids

Liquid	γ_l^d	γ_l^p	γ_l
Water	21.8	51.0	72.8
Formamide	39.5	18.7	58.2
Diiodomethane	48.5	2.3	50.8
Ethylene glycol	26.4	21.3	47.7

3. Results and discussion

3.1. AFM measurements

The image of a bare aluminum sample obtained after immersion in acetone and ethanol is shown in Fig. 4. The surface appears very rough (rms rough = 352 nm) and scratches are clearly visible due to the polishing process.

However, scratches disappear after deposition of the PBA-*b*-PTFEMA coating on aluminum suggesting that the unilayer spreads perfectly on the substrate (Fig. 5). Clearly, the sample surface is relatively homogeneous, with a lower roughness. Some small islands with a diameter of about 1 μm are present on the entire surface and are probably due to the evaporation process of the solvent. This phenomenon has been also reported by To et al. [10] with THF and diblock copolymer poly (styrene-*b*-2-ferrocenylethyl methacrylate) (PS-*b*-PFEMA).

The morphology of the PBA-*b*-PHFEMA sample differs from that of the previous sample. Indeed, the AFM image (Fig. 6) shows a significant porosity over the entire surface. The expansion of the image shows that the pore size is between 0.5 and 1 μm. From this result, it is impossible to conclude about the significance of the pore-depth.

3.2. Contact angle results

The measurement of the contact angle gives information about the wettability of a surface. A drop of a liquid in contact with a solid will adopt a particular shape (spherical), which shows the interaction between
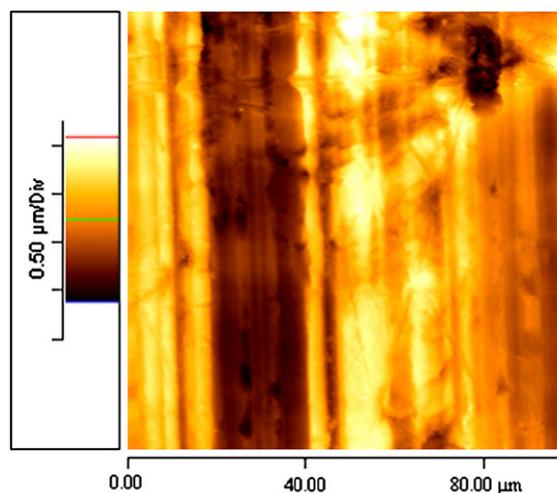

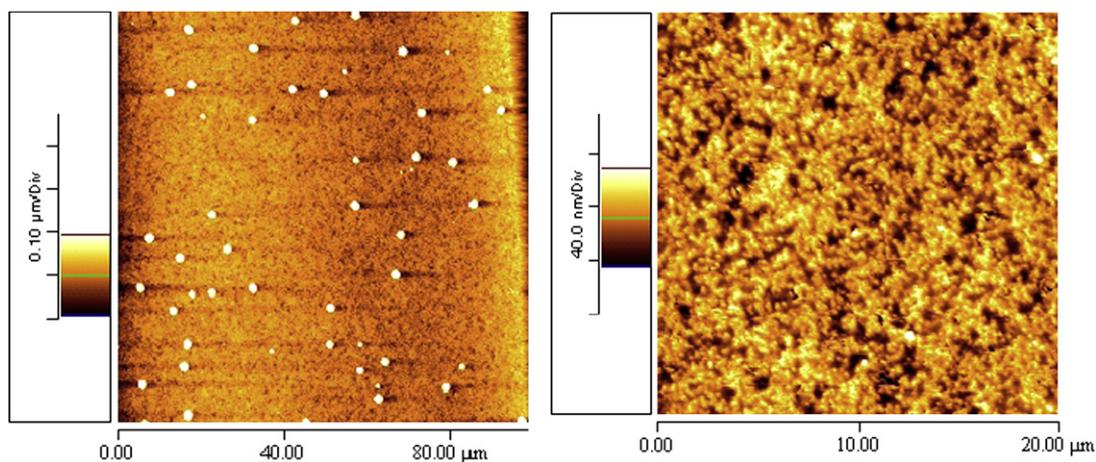Fig. 4. AFM observation of bare aluminium.

Fig. 5. AFM images of PBA-*b*-PTFEMA on aluminium.

the liquid and the solid. The contact angle of the drop with the surface reflects the minimum free energy of the system. The measurement of this angle with water used as a solvent allows deducing the hydrophobic nature (wide angle of contact) or hydrophilic (small contact angle) of the coating. If one uses different kinds of solvents (non-polar and polar), the surface energy of the coating can be deduced using the Owens and Wendt method [9].

The hydrophobicity at the low surface energy properties of fluorinated polymers is well known. In the case of a mixture of polymers, Jones and Kramer [11] have shown that compounds with very low surface energy are very good coating materials. Thus, the comparison of contact angle measurements of each copolymer compared with those obtained for homopolymer can give an indication of the orientation relative to the surface.

3.2.1. Contact angle measurements with water as a solvent

The contact angles measured with water are reported in Table 2. The values of contact angle measurements for the PBA, PTEFEMA and PHEFEMA homopolymers are, respectively, 75, 97 and 120°. Thus the values of the contact angles obtained for the PBA-*b*-PTFEMA and PBA-*b*-PHFEMA coatings are comparable to those of PTFEMA and PHFEMA coatings. One can assume in both cases that the fluorinated blocks are present at the surface of the coating, indicating a preferential orientation of the copolymer.

3.2.2. Surface energy of coatings

The values of polar and non-polar components of the surface energy and the sum of these two components, for all samples, are reported in Table 3.
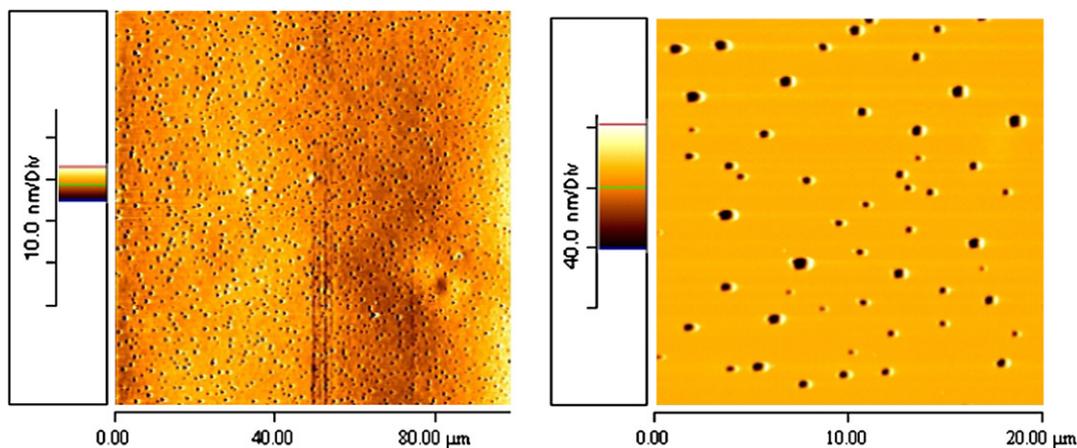

Fig. 6. AFM images of PBA-*b*-PHFEMA on aluminium.

Table 2
Contact angles with water

Polymers	Contact angle (°)
PBA	74
PTFEMA	97
PHFEMA	120
PBA-*b*-PTFEMA (VR 82)	101
PBA-*b*-PHFEMA (VR 89)	120

The surface energy of copolymer PBA-*b*-PTFEMA (18.68 mJ/m^2) is of the order of magnitude of the fluoride PTEFEMA homopolymer (19.92 mJ/m^2). The surface energy of the PBA-*b*-PTFEMA copolymer (18.68 mJ/m^2) is of the order of magnitude of the fluorinated PTEFEMA homopolymer (19.92 mJ/m^2). The same observation can be made for the PBA-*b*-PHFEMA copolymer (8.45 mJ/m^2) and PHEFEMA homopolymer (8.13 mJ/m^2).

These results are in agreement with previous measurements of the angles of contact with water, confirming, in both cases, the preferential orientation of the fluorinated block at the interface between air and coating. It is remarkable that the non-polar component of the surface energy is clearly higher than the polar one, showing the highly non-polar nature of both coatings and, therefore, the hydrophobic behaviour of such a unilayer.

Finally, the surface energy of the PBA-*b*-PHFEMA is lower than that of the PBA-*b*-PTFEMA, indicating a more hydrophobic behaviour. This result is entirely consistent with the fact that the PBA-*b*-PHFEMA copolymer contains a more significant amount of fluorine atoms compared to PBA-*b*-PTFEMA. The decrease in surface energy associated with the increase in the concentration in fluoride atoms is generally fast until a certain value. The hydrophobic properties are maximum when this critical value is reached and cannot be improved with the addition of fluorine atoms [12].

3.3. Impedance results

The barrier properties of an organic coating are very important for its corrosion resistance. The water entering through the coating, even in small quantities, can cause a corrosion reaction at the interface with the metal. The formation of corrosion products can also drastically decrease the adhesion of the coating.

The electrochemical behaviour of an organic coating can be described by different models depending on its porosity. When the layer is perfectly watertight, it can be modelled by an equivalent electrical circuit type R_eQ_c (Fig. 7a), where R_e is the resistance of the electrolyte and Q_c the Constant Phase Element (CPE) of the organic coating. In the case of a fast penetration of electrolyte within the protective layer, the impedance diagrams must then be fitted with a $R_e(R_{po}Q_c)$ circuit type (Fig. 7b), where R_{po} is the resistance of the electrolyte into the pores of the coating.

Finally, if the organic coating contains defects crossing, the contribution from the substrate at the bottom of the defects leads to the following circuit: Re $(R_{po}Q_c (R_tQ_{dl}))$ (Fig. 7c), where R_t and Q_{dl} are, respectively, the charge-transfer resistance and the double layer CPE of the substrate.

Here, Electrochemical Impedance Spectroscopy measurements were carried out in a 3 wt% NaCl solution for durations varying between 60 and 90 days. All impedance diagrams were fitted by choosing the appropriate model among the three models described above.

3.3.1. Evolution of the CPE of the organic coatings and water uptake

The evolution of the organic coating CPE (Q_c) versus immersion time in 3 wt% NaCl for both samples is reported in Fig. 8. All values lie in the same range which is characteristic of an organic coating. While the CPE of the coating PBA-*b*-PTFEMA increases significantly during immersion time, that of PBA-*b*-PHEMA changes very little, even after 60 days of immersion. It is possible to correlate directly the evolution of the CPE of an organic coating to the quantity of electrolyte that penetrates in the coating. For this, the water uptake using the relationship of Brasher and Kingsbury (1) [13] has been determined for each sample (Fig. 9).
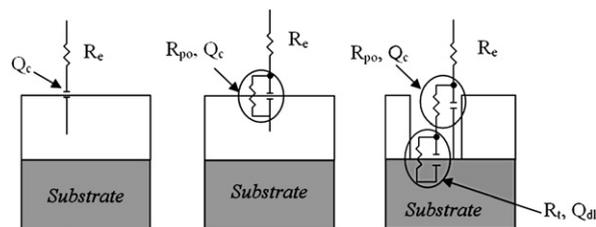
Table 3
Surface free energy of coatings

Polymers	Polar component (A)	Non-polar component (B)	Energies (mJ/m^2) (A + B)
PBA			
PTFEMA	3.16	16.76	19.92
PHFEMA	0.55	7.58	8.13
PBA-*b*-PTFEMA (VR 82)	1.77	16.91	18.68
PBA-*b*-PHFEMA (VR 89)	0.43	8.02	8.45

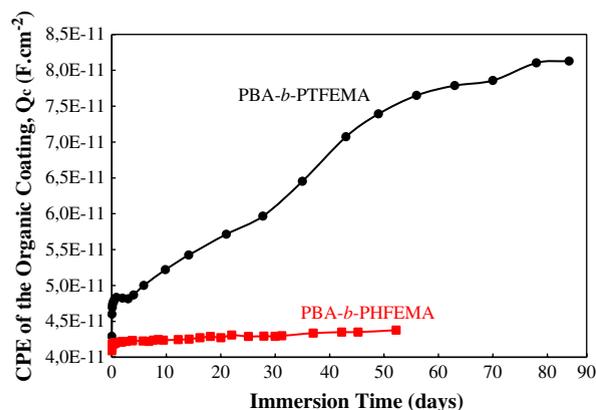Fig. 7. Equivalent electrical circuit models for an organic coating.

Fig. 8. Evolution of the CPE of the organic coating (Q_c) versus immersion time in 3 wt% NaCl.

$$\phi = 100 \; \frac{\log\left(\frac{Q_t}{Q_o}\right)}{\log(\epsilon_w)} \tag{1}$$

with ϕ: the water uptake (in %), Q_o: the CPE value at initial time of immersion of the anhydrous film, Q_t: the CPE at a defined time t, and ε_w: the dielectric constant of water ($\varepsilon_w = 80$, at $T = 20\ °C$).

Thus, one can see that the water uptake of the PBA-*b*-PTFEMA coating is about 14% after 90 days of immersion. This value is very high and shows phenomena more complex than the simple ingress of water into the coating and suggests delamination of the coating. However, the water uptake in the PBA-*b*-PHFEMA coating is slightly modified, remaining below 2% after 60 days of immersion. These results confirm those obtained from contact angle and surface energy measurements, highlighting the more hydrophobic behaviour of the PBA-*b*-PHFEMA coating due to higher concentration in fluorine atoms. Therefore, even if AFM examinations revealed a larger number of holes for the PBA-*b*-PHFEMA sample compared to the
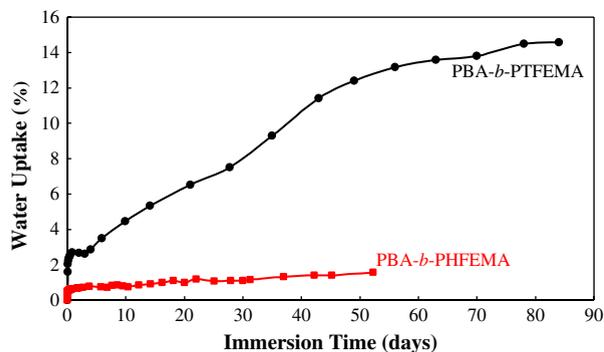

Fig. 9. Evolution of the water uptake in the coatings versus immersion time in 3 wt% NaCl.
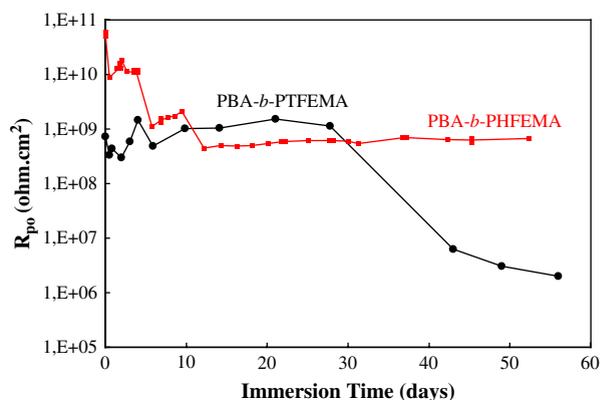

Fig. 10. Evolution of the resistance of the electrolyte in the pores of the organic coating (R_{po}) versus immersion time in 3 wt% NaCl.

PBA-*b*-PTFEMA, this porosity is certainly superficial and does not reach the substrate. The relative high hydrophobicity of the coating can prevent infiltration of the electrolyte through these defects.

3.3.2. Evolution of the barrier effect (R_{po})

A coating is usually considered as protective when the impedance diagram exhibits only one time constant, i.e. when the metallic substrate is not "visible", which corresponds to an R_{po} threshold value of roughly $10^6\ \mathrm{ohm\ cm^2}$. The evolution of the capacitance of an organic coating during the immersion time is directly dependent on the amount of water that has penetrated through the coating. The resistance of the electrolyte into the pores (R_{po}) indicates the presence of defects or diffusion paths until substrate. Thus, a decrease in R_{po} demonstrates the increasingly easy access of the electrolyte to the substrate with all damaging risks as well as delamination of the coating and formation of corrosion products.

The evolution of R_{po} for each sample is presented in Fig. 10. It is apparent that the R_{po} of the PBA-*b*-PTFEMA sample falls rapidly. After 15 days of immersion, R_{po} values are below $10^7\ \mathrm{ohm\ cm^2}$. In contrast, the R_{po} of the PBA-*b*-PHFEMA sample remains high: in the order of $10^9\ \mathrm{ohm\ cm^2}$ even after 60 days of immersion. Clearly, these results confirm the good corrosion barrier properties of the coating based on diblock copolymer PBA-*b*-PHFEMA.

4. Conclusions

Two types of diblock copolymers: poly(*n*-butyl acrylate-*b*-trifluoroethyl methacrylate) diblock copolymer (PBA-*b*-PTFEMA) and an (*n*-butyl acrylate-*b*-heptadecafluorodecyl methacrylate) diblock copolymer (PBA-*b*-PHFEMA) were synthesized by Nitroxide-

Mediated Polymerisation using BlocBuilder™ alkoxyamide initiator. These two copolymers have been used for unilayer-based coatings to protect Al substrates protective against corrosion. The contact angle (with water) and the surface energy measurements have shown in both cases that the fluorinated blocks are present at the surface of the coating, indicating a preferential orientation of the copolymer. The results suggest a higher hydrophobic behaviour of the PBA-*b*-PHFEMA coating due to the higher concentration in fluorine atoms.

Finally, the impedance measurements pointed out the very low penetration of the electrolyte in the PBA-*b*-PHFEMA film (lower than 2%) in contrast to the PBA-*b*-PTFEMA layer (higher than 14%). Due to the very high hydrophobic behaviour and the high resistance of the electrolyte, it has been found that the use of a PBA-*b*-PHFEMA-based unilayer is a promising candidate for blocking corrosion processes on Al after 60 days of immersion.

References

[1] Determination of Coating Performance with Impedance Measurements, TNO Centre for Coatings Research Delft, The Netherlands, 1992.
[2] N.S. Sangaj, V.C. Malshe, Prog. Org. Coat. 50 (2004) 28.
[3] C.M. Hansen, Prog. Org. Coat. 51 (2004) 55.
[4] C.K. Schoff, Prog. Org. Coat. 52 (2005) 21.
[5] L.H. Sperling, Introduction to Physical Polymer Science, J. Wiley & sons, 1992, (Chapter 4).
[6] I.W. Hamley, The Physics of Block Copolymers, Oxford Science Publications, 1998, (Chapter 2).
[7] D. Bertin, M. Destarac, B. Boutevin, Polymers and Surfaces (1998) 47.
[8] D. Benoit, V. Chaplinski, J. Am. Chem. Soc. 121 (1999) 3904.
[9] D.K. Owens, R.C. Wendt, J. Appl. Polym. Sci. 13 (1969) 1740.
[10] T. To, H. Wang, A.B. Djurisic, M.H. Xie, W.K. Chan, Z. Xie, C. Wu, S.Y. Tong, Thin Solid Films 59 (2004) 467.
[11] R.A.L. Jones, E.J. Kramer, Polymer 34 (1993) 115.
[12] K. Li, P. Wu, Polymer 43 (2002) 4079.
[13] D.M. Brasher, A.H. Kingsbury, J. Appl. Chem. 4 (1952) 62.